

A Comparative Study on the 1-D and 3-D Load Follow Analysis Methods of Light Water Reactor

Chang Hyo Kim, Sang Hoon Lee and Chang Hyun Chung

Seoul National University

(Received February 16, 1987)

경수로의 부하추종 운전에 대한 1차원 및 3차원 해석방법의 비교 연구

김창효 · 이상훈 · 정창현

서울대학교

(1987. 2. 16 접수)

Abstract

This work concerns with a comparison of the 1-dimensional (or 1-D) load follow analysis method with reference to the detailed 3-dimensional (or 3-D) computations. For this purpose a 1-D two-group finite difference code, HLOFO, and a 3-D coarse-mesh code based on the modified Borresen's method, CMSNAC, are developed. The CMSNAC code is used to obtain the 3-D power peaks and reactivity parameters in response to power swing from 100 to 50 and back to 100% in the 12-3-6-3 load cycle for the BOL of the KORI Unit 1 PWR core. The 3-D result is then compared with the 1-D HLOFO computations, the cross section and buckling inputs of which are obtained by combining the flux-volume weighting scheme with the approximate flux from the auxiliary 3-D computations. It is shown that the 1-D computation has a limited accuracy, yet it is confirmed that it can describe the core axial average behavior which is fairly consistent with the detailed 3-D computation.

요 약

본 논문은 부하추종운전노심의 1차원 해석방법과 3차원 해석방법을 비교하기 위한 것이다. 이 목적으로 본 논문에서는 유한차분법에 의거한 1차원 HLOFO 코드와 수정형 Borresen 소격모형에 의한 3차원 CMSNAC 코드를 개발했다. CMSNAC 코드는 100-50-100% 출력변화를 수반하는 12-3-6-3 부하추종운전에 대한 고리 1호기 노심의 3차원 출력분포와 반응도 변수를 계산하는데 이용했다. 3차원 계산결과는 중성자속·체적 가중법으로 구한 단면적 및 버클링 입력에 의거한 1차원적 HLOFO 계산결과와 비교되었으며, 이 비교로부터 1차원 HLOFO 계산이 정확도 면에서 다소 뒤떨어지지만 3차원 계산에 가까운 결과를 얻을 수 있다는 것을 보였다.

* This work was supported by the Ministry of Education of the Republic of Korean government.

1. Introduction

As the nuclear fraction of the nation's total electric generation capacity becomes larger, it becomes more important for the nuclear power plants to possess the load-follow capabilities. Studies are under way to investigate the load follow capabilities of the nuclear units in order to determine the feasibility of adopting the load-follow mode as an operational policy.¹⁾ The purpose of this work is to make a comparison of the 1-D and the 3-D methods for the neutronics analysis of the PWR core operating in a load follow mode.

The reactor core in the load-follow operation is subject to frequent changes in the material composition.^{2,3)} Unlike the case of the base-load operation, the control rods frequently move in and out of the core in response to the load change. Soluble boron concentration continues to vary to compensate for the reactivity change arising from varying number density of Xenon and Samarium. These changes in the core composition, especially those by the control rod movement and Xenon number density are asymmetric in the axial direction. It is very likely that they can cause unacceptable local power peaks to occur.

Therefore, the computing system for the load follow analysis should be capable of predicting not only the local power peaks but reactivity parameters including the control rod position, boron concentration and Xenon number density in response to power change. The 3-dimensional code system should be used for the detailed analysis of the load-follow operation, yet it is rather costly due to the long computing time. On the other hand, the 1-dimensional diffusion theory codes have been adopted for the load-follow analysis due to its inherent advantage of good computational efficiency.^{4,5)} Since the

1-D codes describe the core behavior in the sense of the axial average, however, a question has been raised with regard to how the cross section and transverse buckling inputs are prepared to obtain the 1-D results comparable in accuracy to the 3-D results.

Motivated by this fact, the present work investigates the accuracy of the 1-D load-follow analysis method by reference to very detailed 3-D calculations. In doing so, the modified Borresen's coarse-mesh method⁶⁾ is incorporated into a 3-D load-follow analysis code, CMSNAC and a 1-D finite difference diffusion theory code HLOFO is developed. The CMSNAC code is first used to perform the detailed 3-D computation for the power peaks and reactivity parameters in response to power change of KORI Unit 1 PWR, on the assumption that the reactor is subject to the 12-3-6-3 load follow operation on the MINB control strategy. The 3-D result is then compared with the 1-D HLOFO computation in which the cross section and buckling inputs are evaluated using the flux-volume weighting scheme in combination with an auxiliary 3-D flux computation. It is shown that the 1-D computation has a limited accuracy, yet it has been confirmed that the 1-D computation is capable of describing the axial average core behaviour that is consistent with the 3-D results.

2. Description of 1-D and 3-D Methods

The axial power distribution is one of the important reactor parameters in analyzing the PWR core in the load-follow operation. Two computational methods are used in this study: a 3-D coarse-mesh method and a 1-D finite difference method. A brief description for two methods is given below.

2.1. 3-D Coarse-Mesh Method

The theoretical basis for the 3-D load-follow

analysis of the PWR core is a modified scheme of Borresen's 1.5 group diffusion theory method⁷⁾ which is characterized by the nodal coupling relations for the diffusion density of the fast neutron group, $\phi_i = \sqrt{D_{fi}} \bar{\phi}_{fi}$,

$$\begin{aligned} & -\sum_j \phi_j - R \sum_j \phi_j + \frac{p_i + (b + c \cdot r_i) q_i}{1 - c q_i} \\ & = \frac{1}{\lambda} \cdot \frac{V_i}{\sqrt{D_{fi}}(1 - c q_i)} \cdot \\ & \left(\frac{\nu \sum_{fji} \bar{\phi}_{fi} + \nu \sum_{fji} \bar{\phi}_{ji}}{\sqrt{D_{fi}}} \right), \end{aligned} \quad (2-1)$$

where the node-average fast flux, $\bar{\phi}_{fi} = \bar{\phi}_i / \sqrt{D_{fi}}$, is enumerated using an interpolation formula,

$$\bar{\phi}_{fi} = b \phi_{fi} + 2c (\sum_j \phi_{ji}^j + R \sum_j \phi_{ji}^j), \quad (2-2)$$

with the internodal surface flux ϕ_{ji}^j given by the first-order finite difference approximation,

$$\phi_{ji}^j = \frac{D_{fi} \phi_{fi} + D_{fj} \phi_{fj}}{D_{fi} + D_{fj}}. \quad (2-3)$$

The notations in the above have the same meanings in reference 6.

The modified scheme combines Eq. (2-2) with the node-dependent thermal group weighting factors in evaluating the node-average thermal flux, $\bar{\phi}_{ii}$,

$$\bar{\phi}_{ii} = b_{ii} \phi_{ii} + 2c_{ii} \left\{ \sum_j \phi_{ji}^j + R \sum_j \phi_{ji}^j \right\} \quad (2-4)$$

where the b_{ii} and c_{ii} are given by

$$\begin{aligned} b_{ii} &= (1 - 2 \tanh(hK_i/2) / hK_i)^2 \\ & \quad (1 - 2 \tanh(kK_i/2) / kK_i), \\ c_{ii} &= (1 - b_{ii}) / (8 + 4R) \end{aligned} \quad (2-5)$$

In addition, the modified scheme uses an analytical expression for the thermal flux on the interface between node i and j , ϕ_{ij}^j ,

$$\begin{aligned} \phi_{ij}^j &= \frac{\frac{D_{ii} K_i}{T_i} \phi_{ii} + \frac{D_{ij} K_j}{T_j} \phi_{ij}}{\frac{D_{ii} K_i}{T_i} + \frac{D_{ij} K_j}{T_j}}; \\ T_i &= \tanh(K_i h/2) \end{aligned} \quad (2-6)$$

in order to better account for the thermal spectral effects of adjacent nodes in computing ϕ_{ii}^j .

The solution process of Eq. (2-1) involves a

coupled nuclear and thermal iteration due to the fact that the two-group cross section is dependent on such variables as fuel burnup, moderator density, soluble boron concentration, effective fuel temperature, number densities of Xenon-135 and Samarium-149, etc. In addition to the usual inner and outer iterations and criticality search iterations, therefore, iterative recomputation of the power distribution is performed in solving the 1.5 group equation. This iteration continues till one obtains the power distribution which is consistent with that used for generating the cross section inputs.

2.2. 1-D Finite Difference Method

The 1-D finite difference method is designed primarily to determine the axial power distribution. The theoretical basis of the 1-D model adopted in this work is two-group diffusion equation which is given by

$$\begin{aligned} & -D_g \frac{d^2 \phi_g}{dz^2} + (\Sigma_{ag} + D_g B_g^2(z)) \phi_g \\ & = \sum_{g'=1}^2 \left(\frac{1}{\lambda} \nu \Sigma_{fg'} + \Sigma_{sg'} \right) \phi_{g'}. \end{aligned} \quad (2-7)$$

The B_g^2 is the transverse buckling for the g -th group.

There can be many different approaches for obtaining the finite difference approximations to Eq. (2-7). The approach adopted here is to define first 1-D node-average group flux by

$$\phi_{gk} = \frac{1}{h_k} \int_{z_{k-1}}^{z_k} dz \phi_g(z) \quad (2-8)$$

and then to integrate Eq. (2-7) over the axial node k shown in Fig. 1. This approach leads to the so-called three-point difference equation of the box-scheme;

$$a_g^k \phi_{gk-1} + b_g^k \phi_{gk} + c_g^k \phi_{gk+1} = S_{gk} \quad (2-9)$$

where

$$a_g^k = -\frac{r_g^{k-1} \cdot r_g^k}{r_g^{k-1} + r_g^k}, \quad c_g^k = a_g^{k+1}, \quad (2-10)$$

$$b_f^k = (\Sigma_{af}^k + D_f^k B_f^{2k} + \Sigma_r^k) h_k - a_f^k - c_f^k,$$

$$b_i^k = (\Sigma_{ai}^k + D_i^k B_i^{2k}) h_k - a_i^k - c_i^k,$$

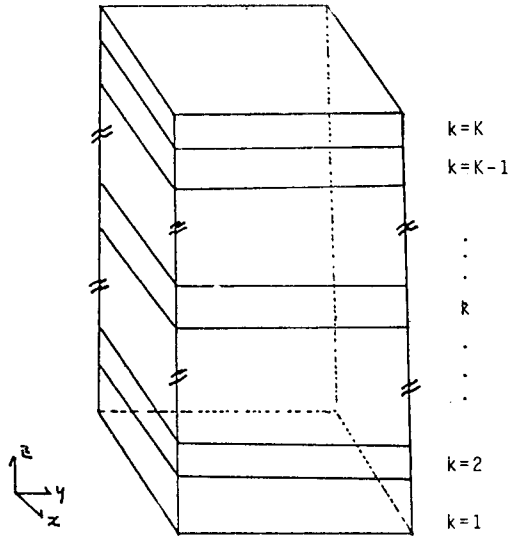


Fig. 1. Axial Node Configuration

$$S_{fk} = \frac{1}{\lambda} (\nu \sum_{ff}^k \phi_{fk} + \nu \sum_{fk}^k \phi_{fk}) h_k,$$

$$S_{tk} = \sum_{fk}^k \phi_{fk} h_k,$$

$$r_g^k = D_g^k / 0.5 h_k$$

The numerical solution to Eq. (2-9) can be obtained by the coupled nuclear and thermal iteration technique mentioned in the 3-D case, once the node-dependent cross section and the transverse buckling B_g^{2k} are known. Thus the problem is how to enumerate the \sum_g^k and B_g^{2k} of the axial nodes so that the 1-D finite difference method can predict the axial power distribution comparable in accuracy to that of the 3-D method.

One simple but straightforward method is the method of the flux-volume weighting⁸⁾ which is expressed by

$$\sum_g^k \phi_{gk} V_k = \sum_{m \in k} \sum_{g \in m} \phi_{gm} V_m,$$

$$D_g^k B_g^{2k} \phi_{gk} V_k = \sum_{m \in k} \sum_{u=x,y} J_{gum} S_{gum} \quad (2-11)$$

where the summation sign stands for the sum over all 3-D nodes contained in the 1-D node. The $J_{gum}(u=x \text{ or } y)$ is the net u -directed currents out of the 3-D node m at the core-reflector

interfaces. The S_{gum} denotes the u -directed nodal surface area of the node m .

3. Numerical Computations and Discussion

The 3-D and 1-D neutronics models just described are incorporated into the computer programs CMSNAC and HLOFO, respectively. They are used for determining some important parameters of a Westinghouse PWR in the load-follow operation; the axial offset, the flux difference, the control rod position, boron concentration, number densities of Xe and Sm. The Westinghouse reactor selected for this computation is the KORI Unit 1.⁹⁾ It is assumed that KORI plant is subject to 12-3-6-3 load cycle (100-50-100% power) at BOL, as shown in Fig. 2 with the MINB control strategy.

Fig. 2 shows the results of 3-D CMSNAC

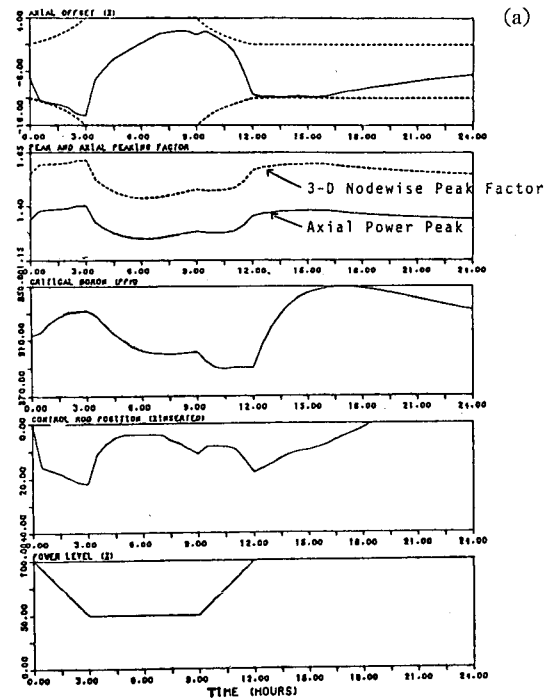


Fig. 2. 3-D CMSNAC Computation for Axial Offset, Power Peaks, Boron Change, and Rod Motion vs. 12-3-6-3 Load Cycle. Two Dotted Lines in (a) stands for Upper and Lower Limits of Target Axial Offsets.

computations for the change of the axial offset, soluble boron concentration, position of D-bank control rods in response to the change of reactor power in 12-3-6-3 load cycle. The computations are performed at the discrete time steps of the 30-minute interval. Fig. 2 shows the typical up and down trends¹⁰⁾ of the control rod position and boron concentration with the change of power in the MINB-mode 12-3-6-3 load cycle. The peaking factor in the 3-D nodewise power distribution is restricted to less than 1.65, so that the pin peaking factor is less than 2.15.

The 3-D computations for the load-follow analysis requires rather lengthy computing time. It is observed that the per step execution time of the CMSNAC program is about 150 seconds on the MV-8000 computer for obtaining the core characteristics in Fig. 2, even with 1 node per fuel assembly on an octant-core symmetry. Thus the completion of the 12-3-6-3 load cycle analysis, which corresponds to a total of 48-step computations, requires the net execution time of about 7,200 seconds.

The 1-D HLOFO computation is designed to get around this drawback of the 3-D computation at the cost of the computing accuracy. Fig. 3 shows a comparison of the 1-D results and the 3-D CMSNAC results for the axial offset and axial peaking factor. The overall agreement of the 1-D and 3-D results are very good, though the axial offset is underestimated a little bit in 1-D results. It should be noted, however, that the 1-D results are obtained using the following assumption and procedure;

- 1) The computing step is taken at the interval of 30 minutes.
- 2) The control rod position and the soluble boron concentration are set at the same value that is used for the 3-D computation every 30-minute interval.
- 3) The cross section and bucklings are obtained combining Eq. (2-11) with the flux

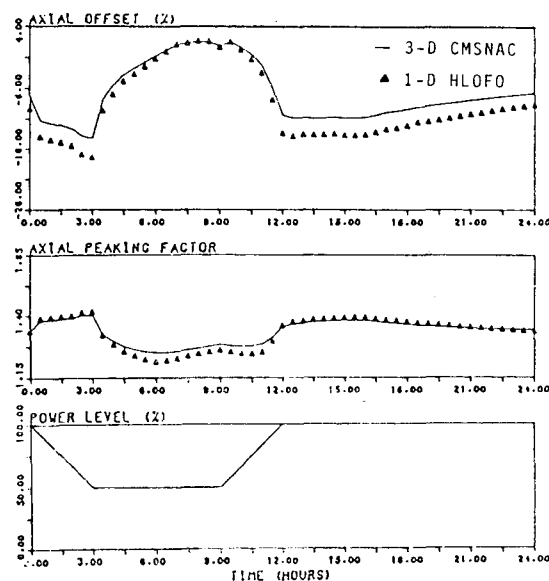


Fig. 3. 1-D HLOFO Computation for Axial Offset, and Axial Power Peaks of the 12-3-6-3 Load Cycle.

and the current from the 3-D CMSNAC computation.

The agreement of the 1-D and the 3-D results as shown in Fig. 3 is presumably the best that can be expected, since the 1-D computation at each time step utilizes the 3-D computations for flux and radial leakage at the corresponding time step. Performing 1-D computation this way is very costly and impractical, since the 3-D computation is required every step 1-D computation is called upon.

In practice, one makes approximation on group flux in preparing the 1-D cross section input and transverse bucklings. The approximation adopted here is to represent the flux to be used in Eq. (2-11) and buckling by a linear-interpolation of the fluxes and bucklings related to four-different core states as shown in Table 1.

The reason for choosing the four states is due to observation that control rods are inserted by 30~50% deep into the core from the top during the 12-3-6-3 load cycle and the power level variation is limited from 100% to 50%. There-

Table 1. Four Core States Used for Approximate Determination of 3-D Flux

core states	flux	transverse buckling
(1) 100% power, ARO	ϕ_{gm}^I	B_{gI}^{2k}
(2) 100% power, ARI	ϕ_{gm}^{II}	B_{gII}^{2k}
(3) 50% power, ARO	ϕ_{gm}^{III}	B_{gIII}^{2k}
(4) 50% power, ARI	ϕ_{gm}^{IV}	B_{gIV}^{2k}

* ARO=All Rods Out and ARI=All Rods In

fore, it is hoped that the mixing of the fluxes corresponding to the four states might approximate the actual flux distribution reasonably well.

Thus the approximate flux to be used in Eq. (2-11) for the cross section of the node k is

$$\bar{\phi}_{gm} = (1-f)(a\phi_{gm}^I + (1-a)\phi_{gm}^{III}) + f(a\phi_{gm}^{II} + (1-a)\phi_{gm}^{IV}). \quad (3-1)$$

As for the transverse buckling,

$$B_g^{2k} = (1-f)(aB_{gI}^{2k} + (1-a)B_{gIII}^{2k}) + f(aB_{gII}^{2k} + (1-a)B_{gIV}^{2k}); \quad (3-2)$$

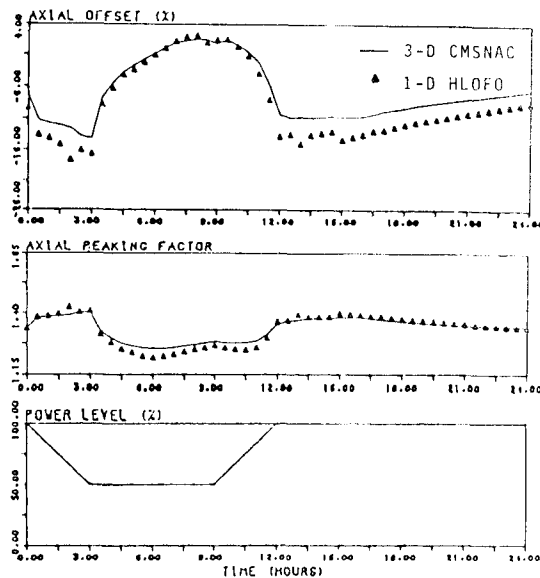


Fig. 4. 1-D HLOFO Computation Using the Cross Section and Buckling Inputs from the Flux-Volume Weighting Scheme with Approximate 3-D Flux.

f = the fraction of control rod insertion into the node k

$$a = (\text{power level} - 0.5) / 0.5.$$

The two-group cross section from the approximate flux, Eq. (3-1), and the approximate transverse buckling from Eq. (3-2) are put into the HLOFO code for the 1-D load follow computation. Shown in Fig. 4 is the 1-D HLOFO computation in comparison with the 3-D CMSNAC computation. It shows that the 1-D results compare well with the 3-D results. For a further comparison, Table 2 presents numerical results of two 1-D computations along with those of 3-D computation. The 1-D results in column 4 of Table 2 differ from those in column 3 in that the former is based on the approximate flux and the approximate transverse buckling given by Eqs. (3-1) and (3-2), while the latter

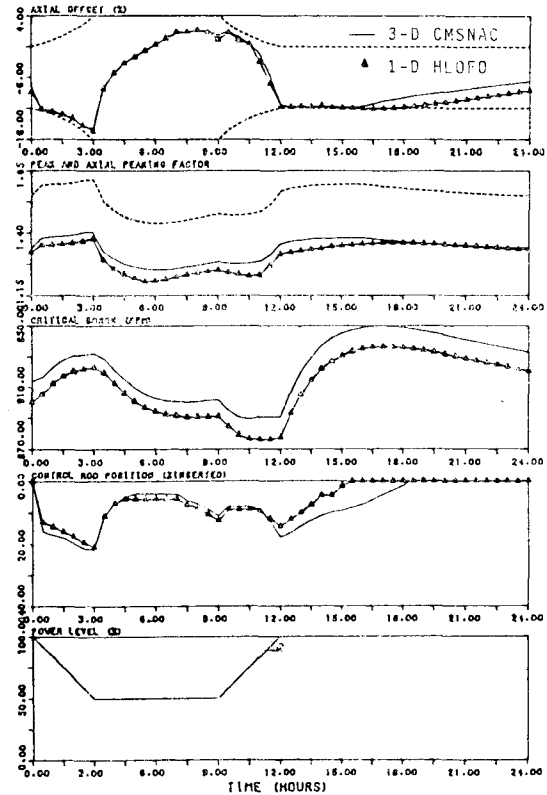


Fig. 5. Comparison of the 3-D CMSNAC and the 1-D HLOFO results for the 12-3-6-3 load follow computation of KORI PWR.

Table 2. Numerical Comparison of the 1-D and the 3-D Load Follow Computations.

time(hr)	3-D model			1-D model					
	A.O.	axial peak	peak node(a)	A.O.	axial peak	peak node(a)	A.O.	axial peak	peak node(a)
.0	-7.24	1.340	9	-9.46	1.334	8	-9.46	1.334	8
1.0	-11.78	1.384	8	-14.67	1.389	8	-14.27	1.384	8
2.0	-12.61	1.390	8	-15.63	1.396	7	-17.74	1.421	7
3.0	-14.30	1.404	8	-17.49	1.415	7	-16.82	1.406	7
4.0	-5.53	1.298	9	-7.12	1.282	8	-6.47	1.276	8
5.0	-2.68	1.264	10	-3.78	1.237	8	-3.48	1.235	8
6.0	-.77	1.252	11	-1.35	1.211	12	-1.15	1.214	9
7.0	1.01	1.256	12	.93	1.225	13	1.06	1.228	13
8.0	1.55	1.269	12	1.45	1.244	13	2.05	1.247	13
9.0	.82	1.285	12	.45	1.259	13	1.33	1.263	13
10.0	.61	1.277	12	.02	1.245	13	.18	1.248	13
11.0	-2.15	1.285	11	-3.57	1.250	10	-4.08	1.254	10
12.0	-10.37	1.355	9	-13.52	1.356	7	-14.02	1.361	7
13.0	-10.72	1.370	8	-13.70	1.375	8	-15.16	1.389	7
14.0	-10.80	1.378	8	-13.73	1.384	8	-13.52	1.380	8
15.0	-10.81	1.381	8	-13.81	1.388	8	-14.54	1.395	8
16.0	-10.69	1.381	8	-13.74	1.389	8	-13.76	1.388	8
17.0	-9.88	1.372	8	-12.80	1.379	8	-13.02	1.381	8
18.0	-9.36	1.366	8	-12.19	1.372	8	-12.16	1.371	8
19.0	-8.77	1.360	9	-11.48	1.363	8	-11.48	1.364	8
20.0	-8.33	1.355	9	-10.89	1.357	8	-10.93	1.357	8
21.0	-7.87	1.351	9	-10.29	1.350	8	-10.31	1.351	8
22.0	-7.44	1.348	9	-9.75	1.344	8	-9.74	1.344	8
23.0	-7.07	1.344	9	-9.20	1.338	8	-9.18	1.338	8
24.0	-6.71	1.342	9	-8.78	1.333	8	-8.75	1.334	8

* A.O.=Axial Offset

(a) The core is discretized into a total of 20 nodes axially. The figure stands for axial node index from the bottom of the core.

is based on the 3-D flux and transverse buckling computed from the 3-D computation at each time interval. Nevertheless, two 1-D results are very similar to each other, which justifies the use of the approximations, Eq. (3-1) and (3-2), in preparing the 1-D HLOFO inputs.

The 1-D inputs prepared from the approximate flux and the transverse buckling are used to compute the axial offset, D-bank control rod position, boron concentration, Xenon and Samarium buildup, etc. of the KORI unit 1 PWR core in response to a 100—50—100% power change in the 12-3-6-3 load cycle on

MINB operation. Fig. 5 depicts the 1-D results with the 3-D CMSNAC results. Overall agreements of two results are remarkably good, though occasional underprediction or overprediction for some core physics parameters are observed in the 1-D results.

4. Conclusion

The load follow analysis of a large PWR core calls for an accurate 1-D code due to its inherent advantage of the fast computing time. The major problem involved in the use of the 1-D

code is how to prepare the cross section inputs and the buckling of the missing dimension. In this work a flux-volume weighting scheme which utilizes approximate fluxes from auxiliary 3-D computations is adopted. It has been shown that this scheme can produce the 1-D results which are fairly consistent with the core axial average of the 3-D CMSNAC computations.

The CMSNAC code developed in this work for the 3-D load follow analysis is very efficient in comparison with other 3-D codes. It has been confirmed⁽¹⁾ that the CMSNAC code is comparable to SIMULATE code in computational accuracy but that it is much faster in computing time than the SIMULATE code. Therefore, the CMSNAC code can serve a useful tool for computing the detailed 3-D power peaks in the rodged and unrodged core with the power history in the load change as well as for confirming the consistency between the core axial average behavior and the 1-D computational scheme.

References

1. S.Y. Park et al., Analysis of Nuclear Power Plant Load Follow Operation by Temperature Reduction Method, J. Kor. Nucl. Soc. 18, 209 (1986).
2. T. Morita and K.J. Dzikowski, Nuclear Design Aspects of Load Following Capability in Westinghouse PWR's, WCAP-8598, Westinghouse Electric Co. (1975).
3. P.J. Sipush et al., Load Follow Demonstrations Employing Constant Axial Offset Power Distribution Control Procedures, Nucl. Tech. 31, 12 (1976).
4. R.F. Barry et al., The PANDA Code, WCAP-7757, Westinghouse Electric Co. (1971).
5. H.J. Moon, DD1D, A One-Dimensional Two-Group Steady-State Neutron Diffusion Theory Program, KAERI/TR-31/18(1981).
6. C.H. Kim, and S.H. Levine, A Modified Borresen Coarse-Mesh Computation for a Three-Dimensional PWR Benchmark Problem, Nucl. Tech. 61, 49 (1983).
7. S. Borresen, A Simplified Coarse-Mesh, Three-Dimensional Diffusion Scheme For Calculating the Gross Power Distribution in a Boiling Water Reactor, Nucl. Sci. Eng. 44, 37(1971).
8. Rudi J.J. Stamm'ler and Maximo J. Abbate, Methods of Steady-State Reactor Physics in Nuclear Design, Academic Press (1983).
9. Nuclear Design Report KORI Unit 1, Cycle 1, Korea Electric Power Company.
10. G.D. Storrick, Generic Load Follow Strategy Report, Korea Electric Power Company.
11. C.H. Kim et al., Development of a Coarse-Mesh Spatial Neutronics Analysis Code of the PWR, CMSNAC (Manuscript in preparation).